

## Evidence for 115 Kilometers of Right Slip on the San Gregorio-Hosgri Fault Trend

**Abstract.** *The San Gregorio-Hosgri fault trend is a component of the San Andreas fault system on which there may have been about 115 kilometers of post-early Miocene right-lateral strike slip. If so, right slip on the San Andreas and San Gregorio-Hosgri faults accounts for most of the movement between the Pacific and North American plates since mid-Miocene time. Furthermore, the magnitude of right slip on a Paleogene proto-San Andreas fault inferred from the present distribution of granitic basement is reduced considerably when Neogene-Recent San Gregorio-Hosgri right slip is taken into account.*

The San Gregorio-Hosgri fault trend parallels the central California coast from its intersection with the San Andreas fault northwest of San Francisco to south of Point Sal (Fig. 1). In this report we present on-land geologic evidence for about 115 km of right-lateral strike slip on this complex fault zone. On-land and offshore segments of the fault trend are well defined by geologic mapping and marine surveys (1-4). Connecting links remain controversial, however, where inferred through shallow water in coastal zones where acoustic profiling data are absent or ambiguous (5-7). Neverthe-

less, chance alignment of several well-defined major faults seems unlikely. Furthermore, if our evidence for right slip on the fault trend is valid, throughgoing continuity of the fault zone is required.

The evidence for right slip consists of seven pairs of offset geologic features (Figs. 1 and 2). None of these are individually unequivocal, but taken together they present a compelling argument. Linear geologic and paleogeographic features forming piercing points on fault planes are the most sensitive indicators of strike slip (8). Certain of the offset pairs listed below are linear features, but unfortunately none are tightly constrained. Consequently, we show probable offset ranges. The common denominator of 115 km (Fig. 2) is our estimate of right slip on the San Gregorio-Hosgri fault trend.

Details of the offset geologic features are presented elsewhere (5, 6), but in summary they include the following.

1) *The Bodega-Gualala fault-Pilarcitos fault offset pair* (asterisks in Fig. 1).

The Pilarcitos fault is an abandoned ancestral strand of the San Andreas fault (9). Although lying west of the modern San Andreas fault, the Pilarcitos fault thus is the local structural boundary between Franciscan Complex on the northeast and granitic basement on the southwest. This pre-San Gregorio fault may be offset to the north as an inferred structural contact separating the northernmost granitic basement outcrops at Bodega Head from the Franciscan-floored (?) latest Cretaceous and early Tertiary Gualala basin west of the San Andreas fault (10).

2) *Point Reyes section-Ben Lomond Mountain section offset* (x's in Fig. 1). Distinctive Tertiary sections, including unconformity-bound packages of Paleocene, middle Miocene, and upper Miocene-Pliocene age, as well as comparable granitic basement, occur at Point Reyes and Ben Lomond Mountain (11-13).

3) *Pigeon Point Formation-Santa Lucia Cretaceous offset pair* (K's in Fig. 1). Upper Cretaceous deep-sea fan deposits of the Pigeon Point Formation (14, 15) and an associated Cretaceous basin margin (6) are probably offset from similar features in the Santa Lucia Range (6). In addition, preliminary studies suggest that Oligo-Miocene shallow- to deep-marine facies overlying the Pigeon Point Formation (16) may have offset equivalents in the Santa Lucia Range (5).

4) *Offset of offshore gravity ridge* (Fig. 1). Silver (17) proposed that a linear gravity feature offshore from Año Nuevo

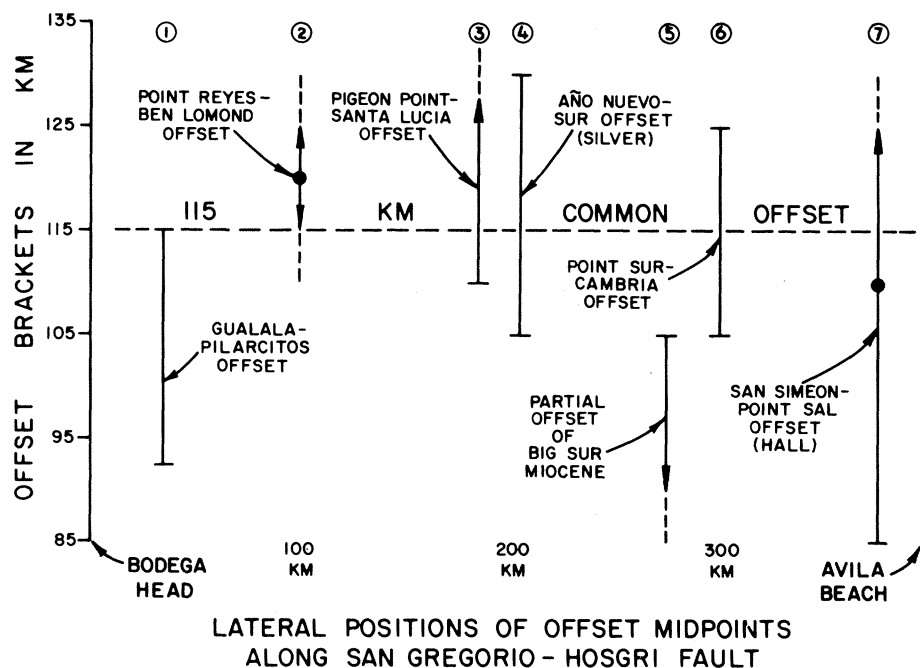
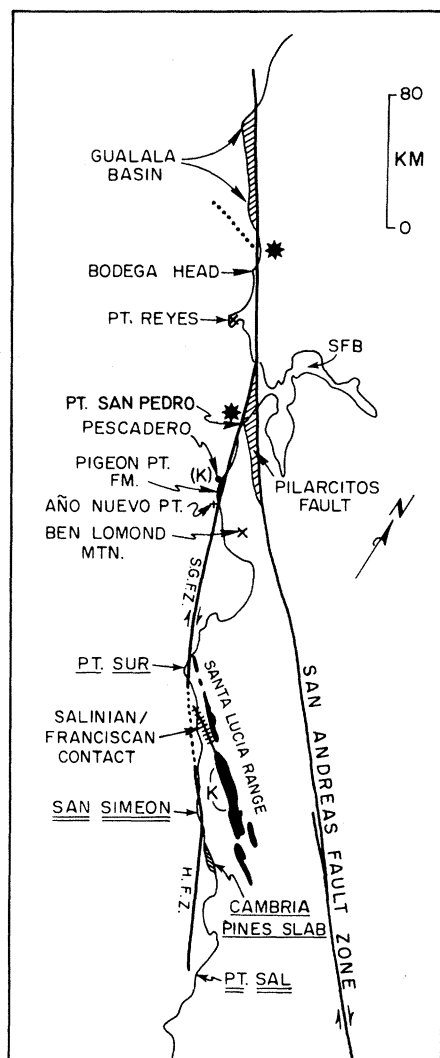


Fig. 1 (left). Map of geologic features offset in a right-lateral sense along the San Gregorio-Hosgri fault trend. See text for discussion. Fig. 2 (right). Offset range chart for suggested offset pairs shown in Fig. 1 and discussed in the text.

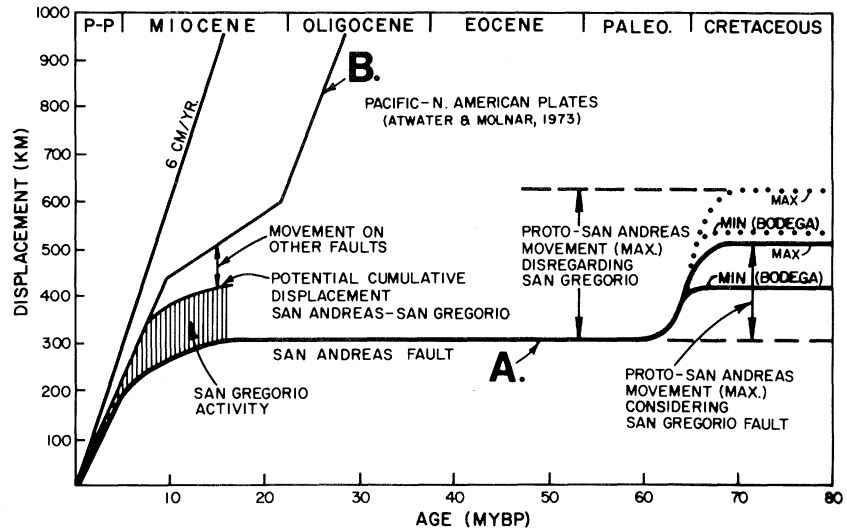
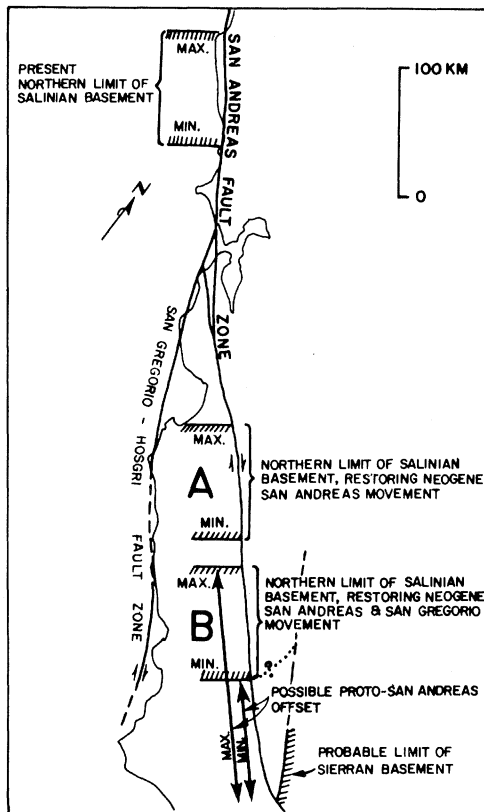


Fig. 3 (left). Northern limit of Salinian block after restoration of Neogene right slip on the San Andreas fault alone (A) or on the San Andreas fault plus the San Gregorio-Hosgri fault trend (B). The remaining offset of granitic basement not accounted for by Neogene right slip may be a measure of right slip on a proto-San Andreas fault. Fig. 4 (right). (Curve A) Time-offset curve (32) modified to show the effect of San Gregorio-Hosgri right slip. (Curve B) Relative motion of the Pacific and North American plates (33). See text for discussion.

Point is the offset expression of the contact between Franciscan rocks and granitic basement of the Salinian block in the Santa Lucia Range.

5) *Point Sur Franciscan-Cambria Pines slab offset pair* (underlining in Fig. 1). The Franciscan subduction complex of the central California coast is generally a potassium feldspar-free metasedimentary sequence (18, 19). Exceptions to this generalization are structural blocks of potassium feldspar-bearing graywacke-shale at Point Sur and Cambria (18, 19). These two blocks apparently have been offset by San Gregorio-Hosgri right slip.

6) *Point Sur Miocene sandstone-Franciscan source terrane offset pair*. Miocene sandstone occupies a small fault slice within the Sur fault zone segment of the San Gregorio-Hosgri fault trend near Point Sur (5, 20). Despite the immediate proximity of granitic basement exposed in Miocene time (5), the sandstone has an exclusively Franciscan provenance (5). At least 60 km of right slip is required to provide an adequate Franciscan source terrane. The offset cannot exceed 105 km, however, because the sandstone lacks volcanic clasts typical of Miocene sandstones near Cambria (21). The lack of overlap of offset between the Point Sur Miocene sandstone and other offset pairs (Fig. 2) does not defeat the offset argument, because the Miocene sandstone is in a fault

slice incorporated in the fault zone at an intermediate distance.

7) *San Simeon ophiolite-Point Sal ophiolite offset pair* (double underlining in Fig. 1). Hall (22) reported the probable offset of a Mesozoic ophiolite and an overlying Tertiary sequence from Point Sal to the San Simeon area along the Hosgri segment of the fault trend.

Displacement of the Point Sal-San Simeon ophiolite association along the Hosgri segment occurred 5 to 13 million years ago (22). Other offset indicators demonstrate post-early Miocene and probable post-middle Miocene right slip. Holocene movement is documented for onland and offshore fault segments (2-4).

Granitic basement of the Salinian block west of the San Andreas fault is offset by a minimum of 510 km, based on northernmost granitic exposures at Bodega Head (Fig. 1). If granitic basement extends offshore to Point Arena (23), the maximum offset is 600 km (Fig. 3). Restoration of well-documented post-Eocene San Andreas right slip of 305 km (24-26) brings the northern limit of Salinian basement back to position A in Fig. 3. The difference between position A (Fig. 3) and the northwest limit of Sierran basement has been taken as a measure of pre-Eocene "proto-San Andreas" right slip (27, 28). Other regional evidence places this deformation in Paleocene time (5, 29). However, the resto-

ration fails to consider the extension of Salinian basement by 115 km of San Gregorio-Hosgri right slip north of its intersection with the San Andreas fault (22, p. 1293). The restoration of this additional 115 km of Neogene to Recent right slip to position B (Fig. 3) reduces by one-third or perhaps two-thirds the apparent right-slip offset of the northern limit of the Salinian block by the supposed proto-San Andreas fault. Furthermore, in the unlikely event that the limit of Sierran basement actually lies to the north in the subsurface (30), and if Bodega Head is near the northern limit of Salinian granitic basement, then a proto-San Andreas fault is precluded along the modern San Andreas pathway in central California. In any event, the proto-San Andreas fault apparently was not a transform fault analogous to the modern San Andreas fault system. Instead, proto-San Andreas faulting may have been the geologic resolution of oblique subduction along the central California coast in early Tertiary time (31).

Right slip of the San Andreas fault is conveniently displayed as a time-displacement plot on curve A in Fig. 4 (32). The dotted modification of curve A prior to 60 million years ago shows the effect of disregarding San Gregorio-Hosgri right slip in proto-San Andreas fault interpretations. Curve B in Fig. 4 shows the relative movement between the Pacific and North American plates (33).

Within the uncertainty of the curves, most movement between the plates has been localized along the San Andreas fault proper for the last 6 million years. Between that time and the early Miocene, most of the plate motion was distributed between the San Andreas and San Gregorio-Hosgri fault trends. Thus the present extension of granitic basement of the Salinian block in large part is explained by right slip on faults of the Neogene San Andreas fault system, as suggested by Johnson and Normark (34).

S. A. GRAHAM

Exploration Department, Western Region, Chevron U.S.A. Inc., San Francisco, California 94119

W. R. DICKINSON

Department of Geology, Stanford University, Stanford, California 94305

#### References and Notes

1. A. K. Cooper, *U.S. Geol. Surv. Open File Rep. 1907* (1973), p. 65.
2. G. E. Weber, *Geol. Soc. Am. Abstr. Programs* **9**, 524 (1977).
3. H. G. Greene, W. H. Lee, D. S. McCulloch, E. E. Brabb, *U.S. Geol. Surv. Misc. Field Stud. Map MF-518* (1973).
4. H. C. Wagner, *U.S. Geol. Surv. Open File Rep.* (1974).
5. S. A. Graham, dissertation, Stanford University (1976), p. 510.
6. \_\_\_\_\_ and W. R. Dickinson, *Calif. Div. Mines Geol. Spec. Rep.*, in press.
7. E. A. Silver, *Geol. Soc. Am. Abstr. Programs* **9**, 500 (1977).
8. J. C. Crowell, *Geol. Soc. Am. Spec. Pap.* **71** (1962), p. 61.
9. For example, see T. H. Nilsen and T. R. Simoni, Jr., *J. Res. U.S. Geol. Surv.* **1**, 439 (1973).
10. C. M. Wentworth, *Stanford Univ. Publ. Geol. Sci.* **11**, 130 (1968).
11. A. J. Galloway, *Calif. Div. Mines Geol. Bull.* **202** (1977).
12. J. C. Clark, dissertation, Stanford University (1966).
13. D. C. Ross, *U.S. Geol. Surv. Prof. Pap.* **698** (1972).
14. J. C. Crowell, *Geol. Soc. Am. Bull.* **68**, 993 (1957).
15. D. R. Lowe, *Proc. 24th Int. Geol. Congr.* **6**, 75 (1972).
16. J. C. Clark and E. E. Brabb, *Calif. Div. Mines Geol. Spec. Rep.*, in press.
17. E. A. Silver, *Geol. Soc. Am. Abstr. Programs* **6**, 253 (1974).
18. W. Gilbert, *Geol. Soc. Am. Bull.* **84**, 3317 (1973).
19. K. J. Hsu, *Calif. Div. Mines Geol. Spec. Rep.* **35** (1969).
20. P. D. Trask, *Bull. Dep. Geol. Univ. Calif.* **13**, 133 (1926).
21. C. A. Hall, Jr., *U.S. Geol. Surv. Misc. Field Stud. Map MF-599* (1974).
22. \_\_\_\_\_, *Science* **198**, 1291 (1975).
23. E. A. Silver, J. R. Curray, A. K. Cooper, in *Geologic Guide to the Northern Coast Ranges, Point Reyes Region, California*, J. H. Lipps and E. M. Moores, Eds. (Geological Society, Sacramento, Calif., 1971), vol. 1, pp. 1-10.
24. W. R. Dickinson, D. S. Cowan, R. A. Schweickert, *Am. Assoc. Pet. Geol. Bull.* **56**, 375 (1972).
25. V. Matthews, III, *ibid.* **60**, 2128 (1976).
26. T. H. Nilsen and M. H. Link, in *Paleogene Symposium*, D. W. Weaver, G. Hornaday, A. Tipton, Eds. (Society of Economic Paleontologists and Mineralogists, Tulsa, 1975), p. 367.
27. J. Suppe, *Geol. Soc. Am. Bull.* **81**, 3253 (1970).
28. R. W. Kistler, Z. E. Peterman, D. C. Ross, D. Gottfried, *Stanford Univ. Publ. Geol. Sci.* **8**, 339 (1973).
29. For example, see S. A. Graham, *Neogene Symposium*, A. E. Fritsche, H. Ter Best, Jr., W. W. Wornardt, Eds. (Society of Economic Paleontologists and Mineralogists, Tulsa, 1976), p. 125.
30. See the dotted line in Fig. 3.
31. P. J. Coney, *Geol. Soc. Am. Spec. Pap.*, in press.
32. Modified from the curves of Dickinson *et al.* (24) and Nilsen and Link (26) in accordance with a Miocene-Pliocene boundary near 5 million years ago. For a detailed discussion see Graham (5).
33. T. Atwater and P. Molnar, *Stanford Univ. Publ. Geol. Sci.* **13**, 136 (1973).
34. J. D. Johnson and W. Normark, *Geology* **2**, 11 (1974).
35. Our research was supported in part by the Earth Science Section, National Science Foundation (grant DES72-01728).

23 May 1977; revised 22 August 1977

3-day period on *lmlm* milk. Nevertheless, pups of all ages display reduced weight and fur development when nursed on *lmlm* milk.

In an attempt to determine the cause of death, tissue sections from the affected pups were examined histologically. Thin sections of skin, lung, liver, stomach, bone, and muscle were prepared from 8-day-old pups nursed on *lmlm* milk. The sections were stained with hematoxylin and eosin and examined under the light microscope. Only the skin appeared abnormal, displaying focal acute dermatitis, general underdevelopment, and follicle atrophy. Furthermore, the stratum granulosum was significantly thickened and the number of hair shafts markedly reduced. All other organs appeared normal, though undersized, and no evidence of infection, allergy, or incomplete digestion of milk was observed.

Histological observations were also made of mammary glands of *lmlm* dams whose pups were close to death. In general, these glands appeared less active and smaller than those of normal B/6 mice. Moreover, we observed that *lmlm* dams frequently yield less milk.

Taken together, these symptoms are similar to those described by Mutch and Hurley (3) in rat pups nursed on dams receiving a postgestational zinc-free diet. This diet leads to a 50 percent decrease in the zinc content of the milk by day 18 of lactation, with only minimal effects on the other constituents. As a result, nursing pups are severely depleted of plasma zinc. Two-thirds of such animals die and all exhibit retarded growth and severe dermatitis. Moreover, total milk production was reduced by 50 percent in the zinc-deficient dams.

Because of the similarity of symptoms between the dietary-induced zinc deficiency and the *lethal milk* syndrome, we compared the concentrations of zinc in the milk of *lmlm* and normal mice. As shown in Table 1, the zinc content of the milk of mutant mice is reduced 34 percent from that of normal B/6 mice. This difference is seen throughout lactation and is reflected in the whole body zinc concentrations of 8-day-old suckling animals. However, we found no such deficiency in either the plasma of lactating *lmlm* dams or in the carcasses of adult *lmlm* females. Since adult *lmlm* females exhibit normal concentrations of total body zinc, it appears that the mutation involves reduced transport of zinc from plasma to milk. The B/6 dams maintain a zinc concentration in the milk that is ten times higher than that in the plasma,

## Zinc Deficiency in Murine Milk Underlies Expression of the *Lethal Milk (lm)* Mutation

**Abstract.** *The inability of nursing pups to survive on milk of mice homozygous for the recessive mutation, lethal milk (lm), is correlated with a reduction in zinc levels of both milk and pup carcass. Administration of zinc to pups nursing on lmlm dams reduces the observed mortality and morbidity. It is suggested that lm alters zinc transport from maternal blood to milk and that its study may provide useful information for understanding the rare human disease, acrodermatitis enteropathica.*

A recessive mutation, designated *lethal milk (lm)*, was discovered among mice of the C57BL/6J (B/6) strain (1). Pups nursed on *lmlm* dams exhibit stunted growth, acute dermatitis, alopecia, and death prior to weaning. Since normal B/6 pups (*LmLm*) die when nursed on *lmlm* milk, the defect resides in the milk. Moreover, *lmlm* pups develop normally if foster-nursed on a normal dam. Genetic analyses indicate that *lm* is located on chromosome 2 and maps 9.6 centimorgans from the agouti (*a*) locus.

The effects of *lmlm* milk on newborn

pups persist at all stages of lactation (2). We have confirmed that newborns fostered on *lmlm* dams at mid-lactation or late lactation are as severely affected as those nursed from the beginning of lactation. In addition, we have found a difference in susceptibility to the effects of *lmlm* milk with respect to the age of pups. Newborn pups are irreversibly committed to death after 3 days on *lmlm* milk, even when subsequently transferred to a normal dam. Older pups, on the other hand, having nursed on normal milk for a few days, frequently survive a